PAPER

Detection limits of organic compounds achievable with intense, short-pulse lasers†

Cite this: DOI: 10.1039/c5an00529a

Jordan Miles,[a] Simone De Camillis,[a] Grace Alexander,[a] Kathryn Hamilton,[a] Thomas J. Kelly,[b] John T. Costello,[b] Matthew Zepf,[a] Ian D. Williams[a] and Jason B. Greenwood*[a]

Many organic molecules have strong absorption bands which can be accessed by ultraviolet short pulse lasers to produce efficient ionization. This resonant multiphoton ionization scheme has already been exploited as an ionization source in time-of-flight mass spectrometers used for environmental trace analysis. In the present work we quantify the ultimate potential of this technique by measuring absolute ion yields produced from the interaction of 267 nm femtosecond laser pulses with the organic molecules indole and toluene, and gases Xe, N_2 and O_2. Using multiphoton ionization cross sections extracted from these results, we show that the laser pulse parameters required for real-time detection of aromatic molecules at concentrations of one part per trillion in air and a limit of detection of a few attomoles are achievable with presently available commercial laser systems. The potential applications for the analysis of human breath, blood and tissue samples are discussed.

Introduction

The potential for using resonantly enhanced multiphoton ionization (REMPI) to detect trace amounts of organic molecules has been recognized for at least 35 years.[1–3] By using ultraviolet laser pulses which are resonant with allowed transitions in the molecules, extremely efficient, soft ionization is possible allowing identification in a mass spectrometer with a sensitivity which theoretically approaches the single molecule limit.

To date the potential of this technique has mainly been investigated using low repetition rate nanosecond lasers as the ionization source. A straightforward way to efficiently ionize aromatic molecules is to use the fourth harmonic of a Nd:YAG laser (266 nm) for resonant ionization *via* a 1 + 1 photon absorption scheme. A wider range of molecules can be accessed using shorter wavelengths (*e.g.* fifth harmonic) or an optical parametric oscillator (OPO). The wavelength tunability of an OPO can also enhance the signal and species selectivity if specific peaks in the absorption spectrum can be picked out. This can be further optimized if the gas is cooled in a jet expansion to limit transitions from excited vibrational and rotational levels of the ground electronic state.[4] This Jet-REMPI scheme is very useful in complex samples as it also allows isobars and isomers to be clearly identified, for example xylenes[5–7] and xylenols.[8] The pulsed nature of these sources makes them ideally suited for integration into time-of-flight (ToF) mass spectrometers.

Since the typical laser intensities are well below that required for non-resonant ionization of background gases, very high sensitivities can be obtained from direct analysis of gas samples without pre-concentration. As a result REMPI has been employed in a number of environmental monitoring studies, particularly in the study of the chemical composition of the exhaust gases from combustion processes such as waste incineration,[6,7,9,10] and engines or generators[4,5,11] (see Streibel and Zimmermnn for a recent review[12]). These studies have demonstrated that an extensive range of volatile organic compounds (VOCs) such as simple aromatics[4–6,10,11,13] aldehydes,[4,14] amines,[15] polychlorinated biphenyls (PCBs),[14,16,17] poly-aromatic hydrocarbons (PAHs)[5,9–11] and dioxins[18] can be detected at parts per trillion (ppt) concentration levels.

This direct sampling, high sensitivity approach could also make Jet-REMPI-ToF valuable for characterizing human breath, which is being widely investigated and promoted as a non-invasive diagnostic for a range of diseases, particularly cancer. Short *et al.*[19] have demonstrated that wavelength selective resonant ionization enables the nitric oxide concentration of human breath to be monitored in real time with ppb sensitivity. Oser *et al.*[20] have also detected a range of aromatic molecules which are potential disease biomarkers with sensitivities nearly two orders of magnitude greater than that achievable

[a]*Centre for Plasma Physics, School of Maths and Physics, Queen's University Belfast, BT7 1NN, UK. E-mail: j.greenwood@qub.ac.uk*
[b]*School of Physical Sciences and National Centre for Plasma Science & Technology, Dublin City University, Dublin 9, Ireland*
†Electronic supplementary information (ESI) available. See DOI: 10.1039/c5an00529a

with a conventional gas chromatograph-mass spectrometer (GC-MS). Given these promising preliminary results it is surprising that many more studies have not been forthcoming. This might be attributed to a reluctance to utilize lasers which are costly, bulky and require operational expertise in a medical setting.

For solid and liquid samples, ns-REMPI has also been used as an ionization source in GC-MS-ToF instruments. For instance it was shown to be superior to electron impact ionization for identifying PAHs in river water samples since there was less molecular fragmentation and better selectivity.[21,22] Alternatively the third harmonic of Ti:sapphire femtosecond lasers (267 nm) has also been used since it gives higher ionization efficiency for molecules with intermediate excited states possessing short lifetimes. For example, excited singlet states of dioxins undergo rapid inter-system crossings to lower lying triplet levels, but using a fs laser allows sample sizes in the femtogram range to be measured.[23–25]

As the size of the molecule increases, more pathways for redistribution of the excitation energy become available. As a result the ionization efficiency is expected to drop for ns lasers and there is an increased degree of fragmentation. This is due to a transition from a ladder climbing process to a ladder switching one where evolution of intermediate excited states opens up many more dissociation channels, thus emphasizing the advantage in using femtosecond pulses for more complex molecules. This was demonstrated in a study comparing the spectra and ionization yields of peptides by fs and ns lasers operating at 267 nm.[26] For compounds lacking conjugated double bonds, absorption bands are deeper in the UV. As a result using the fourth (200 nm) rather than the third harmonic of a Ti:sapphire laser was found to enhance the limit of detection for a large number of pesticides by up to two orders of magnitude.[27]

Non-resonant ionization using femtosecond lasers has also been considered for analysis of organic compounds due to the high ionization efficiency and low molecular fragmentation.[28–31] In the tunneling ionization regime there is a strong dependence on the ionization potential which favors ionization of the organic molecules compared with the main gases found in air. However, it is well established that ionization rates for most organic molecules are suppressed compared to atoms with similar ionization potentials.[32] This depends on the nature of the electronic orbital being ionized which can lead to destructive interference in the outgoing wavepackets which suppress the ionization.[33–35] Therefore, fs lasers which are non-resonant are unlikely to achieve the highly selective ionization required to detect organic molecules at very low concentrations, but could be used in cases where very high efficiency is required, *e.g.* post-ionization in secondary ion mass spectrometry.[36]

Despite the fact that resonant and non-resonant multiphoton ionization offers superior efficiency, lower molecular fragmentation, and higher selectivity than other ionization sources, applications described above have been relatively limited to date. This is mainly due to the cost and expertise associated with using the high peak power lasers required for ionization. However, short pulse laser technology has advanced beyond recognition since REMPI analysis was first proposed. In recent years there have been further dramatic developments in picosecond and femtosecond solid state and fibre lasers based on erbium and ytterbium doped materials. The very high quantum efficiencies of these compounds and the fact that they can be pumped with light emitting diodes rather than separate lasers means that these compact, turnkey and robust devices are now widely used in material processing, telecommunications, medicine and in many research applications. As a result the footprint and price of these lasers has concomitantly been falling rapidly, opening up the possibility of greater exploitation in trace chemical analysis.

In this paper we assess the merits of using commercially available high average power, short pulse lasers for detecting aromatic compounds at ultralow concentrations. We gauge the relative merits of laser parameters such as repetition rate, pulse energy, beam size, and pulse length on the ionization efficiency of analyte molecules and background gases. To compare the relative ionization efficiencies of exemplar aromatic molecules to other gases, we have measured absolute ion yields using a simple ToF device described in section 2. In section 3 we formulate the ion yields expected for the multiphoton ionization and in section 4 present the experimental ion yields produced from 267 nm, femtosecond pulse interactions with indole, toluene, Xe, N_2 and O_2 for a range of intensities. Although we use the organic molecules primarily as exemplars, their trace detection is of particular interest since indole has been demonstrated as a marker for stress in humans[37] and elevated levels of toluene in human breath have been correlated with lung cancer and smoking.[38,39] From these results the laser parameters required to detect 1 ppt concentrations in air are estimated in section 5. Section 6 summarizes these results and also considers the ideal laser characteristics for ultra-high sensitivity detection, the technological developments which might enhance this further, and the potential applications in medicine and trace analysis.

Experimental setup

The ultraviolet laser pulses used to ionize various gases were produced from the third harmonic conversion of a Coherent Inc. Libra titanium:sapphire laser operating at 1 kHz. The resulting pulses had a central wavelength of 267 nm with a bandwidth of 1 nm, pulse energies of 50 μJ, and 130 fs duration (measured from cross correlation with the fundamental). To obtain ion yields as a function of the peak intensity, pulses were attenuated by rotating a half waveplate placed in front of a Glan-Laser polarizer. The pulses were focused by a spherical lens (f = 0.175 m) into the extraction region of a small, home built ToF mass spectrometer.

The interaction region of the ToF consisted of a repeller plate held at a potential of +5 kV with a 5 mm gap to an extraction plate at +4.7 kV. A glass cylinder with a resistive inner coating and 35 mm length was used to generate a uniform

electric field between the extraction plate and a grounded flight tube of 280 mm length. To measure the absolute ion yield per laser shot, a flat stainless steel disc was connected to a low noise charge sensitive amplifier (Amptek CoolFET) which had previously been calibrated absolutely.[40] As a result of the image charge produced by the ions as they approach this plate, the time resolution of this detector was modest but sufficient to separate the ions being studied. The acceptance aperture to the flight tube of diameter L = 10 mm was much greater than the Rayleigh length z_0 of the focused laser beam. To obtain single ionization yields for molecular species, dissociative ionization was included by summing the contributions from fragments as well as the parent ions.

A constant target density was achieved by flooding the chamber with the target gas. The pressure was monitored with an ion gauge and the relative densities of each gas were obtained by correcting for the ion gauge sensitivity. For O_2, N_2 and Xe standard correction factors were used, while factors for toluene and indole were derived from the ratio of their electron impact ionization cross sections (at 100 eV) to that of N_2.[41,42]

Ion yield simulations

For resonantly enhanced 1 + 1 ionization with photons of energy $\hbar\omega$, if the rate of excitation from the ground to excited state is $\Gamma_1(I)$ and the rate of ionization from the excited state to the continuum is $\Gamma_2(I)$ where I is the laser intensity, then the probability of ionization P_{1+1} after a time t is (see ESI†)

$$P_{1+1} = 1 - \frac{\Gamma_2\Gamma_1}{\Gamma_2 - \Gamma_1}\left[\frac{1}{\Gamma_1}\exp(-\Gamma_1 t) - \frac{1}{\Gamma_2}\exp(-\Gamma_2 t)\right] \quad (1)$$

Assuming the laser has a rectangular temporal profile of length τ, and the intensity is sufficiently low so that $P \ll 1$, the ionization probability in terms of the respective cross sections σ is;

$$P_{1+1}(I) = \frac{1}{2}\sigma_1\sigma_2\left(\frac{I}{\hbar\omega}\right)^2\tau^2 \quad (2)$$

This equation assumes that the lifetime of the excited state is much longer than the laser pulse length and that its evolution during the pulse does not influence the value of σ_2. Depending on the strength of the excitation, σ_1 could have values in the range 10^{-16}–10^{-20} cm^2. Absolute values for a number of volatile organic compounds in the gas phase are available in the literature[43–47] or can be estimated from molar absorptivities ε *via* the following conversion

$$\sigma_1\ (\mathrm{cm}^2) = 3.82 \times 10^{-21}\varepsilon\ (\mathrm{l\ mol^{-1}\ cm^{-1}}) \quad (3)$$

Ionization cross sections are only known in a few cases,[3] but are generally of the order of 10^{-17} cm^2 and are not expected to change dramatically with wavelength or the rovibrational state of the excited level.

For the case of non-resonant ionization *via* N photon absorption, the ionization probability is

$$P_N(I) = 1 - \exp\left(-\sigma_N\left(\frac{I}{\hbar\omega}\right)^N t\right) \quad (4)$$

where σ_N is the N photon ionization cross section (units cm^{2N} s^{N-1}).

Values for σ_N are rarely known, but the cross section for 3 photon ionization of xenon at a wavelength of 266 nm has been calculated by Kulander *et al.*[48] to be 2.5×10^{-82} cm^6 s^2, while McGuire *et al.*[49] obtained a value of 5×10^{-82} cm^6 s^2. In order to estimate ionization cross sections from our experimental ion yields and to predict ion yields from hypothetical gas analysis scenarios, we consider theoretical ion yields from the interaction of the laser beam with a gas target of constant number density n. For a tightly focused beam with a Gaussian spatial profile and Rayleigh length $z_0 \ll L$, the total ion yield Y from a pulse of peak intensity I_0 is obtained by integrating the ionization probability over the focal volume (see ESI†)

$$Y(I_0) = \frac{nV_0}{3}\int_{I_{\min}}^{I_0}\frac{P(I)}{I}\left(\frac{I_0}{I} - 1\right)^{1/2}\left(\frac{I_0}{I} + 2\right)\mathrm{d}I \quad (5)$$

For a given ionization probability function $P(I)$ (eqn (1) or (4)), this can be numerically integrated for different peak intensities. As the ionization probability approaches 1, the ion yield keeps increasing due to the increase in iso-intensity volumes which scale as $I^{3/2}$ (see ESI†).

For the other extreme where the laser beam area is constant over an interaction length L (*e.g.* an unfocussed beam) and assuming it has a full width half maximum diameter of D, pulse length τ, and pulse energy E, the integrated ion yield $Y_{N=3}$ from this interaction is determined to be (see ESI†)

$$Y_3 = \frac{16(\ln 2)^2 \mathrm{Ln}\sigma_3}{3\pi^2(\hbar\omega)^3 D^4}\frac{E^3}{\tau^2} \quad (6)$$

By similar analysis the yield from resonant 1 + 1 ionization is;

$$Y_{1+1} = \frac{(\ln 2)\mathrm{Ln}\sigma_1\sigma_2}{(\hbar\omega)^2\pi D^2}E^2 \quad (7)$$

Results

The Xe^+ ion yield generated per laser pulse at the focus of the beam, normalized to an absolute gas pressure of 10^{-7} mbar, as a function of peak intensity I_0 is shown in Fig. 1(a). Calibration of the intensity scale was obtained by using the cross section of 2.5×10^{-82} cm^6 s^2 calculated by Kulander *et al.*[48] and fitting eqn (5) to the experimental ion yield. To extend the measurements to lower intensities (~10^{12} W cm^{-2}), data was also acquired with the laser focus shifted 18 mm off the ToF axis. These points were corrected for the increased interaction volume and included on Fig. 1(a). Trend lines are also plotted which confirm the expected $I^{3/2}$ and I^3 dependencies for Xe well above and below the saturation intensity respectively.

The yields for N_2 and O_2 are also shown in Fig. 1(a) having been normalized to the same target density as Xe. Similar trends are found for both but with lower yield and higher saturation intensities compared to Xe. The fact that the yield of

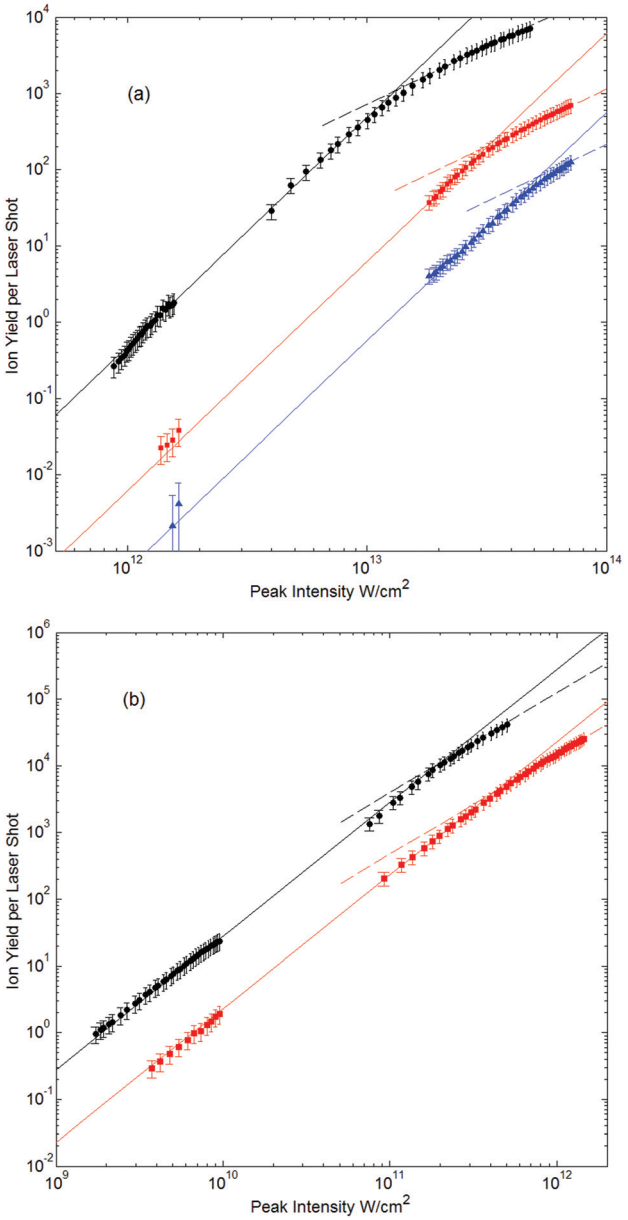

Fig. 1 Ion yield per laser shot as a function of peak pulse intensity for 130 fs, 267 nm pulses normalized to an absolute gas pressure of 10^{-7} mbar. (a) Xe (black circles), N_2 (red squares) and O_2 (blue triangles); (b) indole (black circles) and toluene (red squares). Dashed lines show $I^{3/2}$ trends, solid lines show (a) I^3 and (b) I^2 trends.

ions from N_2 follows an I^3 trend at low intensities is surprising given that four photons are required for ionization. This indicates the presence of strong resonances around 14 eV above the N_2 ground state.[50] By fitting eqn (5) to the data, three photon cross sections of 1.8×10^{-83} cm^6 s^2 and 3.5×10^{-84} cm^6 s^2 for O_2 and N_2 were derived with an uncertainty of 40%.

As indole and toluene are considerably easier to ionize, the same off focus interaction geometry was used to obtain ion yields around the saturation intensity. These results are shown in Fig. 1(b) along with yields for much lower intensities

Table 1 Cross sections (cm^2) used to fit the data in Fig. 1(b)

	Indole	Toluene
Excitation σ_1 [51,52]	1.0×10^{-17}	1.3×10^{-18}
Ionization σ_2	2.0×10^{-17}	1.4×10^{-17}

obtained using an unfocussed beam (which was again corrected to account for the different interaction geometry). These results follow the expected intensity dependencies of $I^{3/2}$ and I^2 above and below saturation intensities of 2.0×10^{11} W cm^{-2} and 4.5×10^{11} W cm^{-2} for indole and toluene respectively. The excitation cross section for toluene has been measured previously in the gas phase,[51] while the value for indole can be derived from its molar absorptivity in solution.[52] The 0–0 transition in toluene is at 272 nm while at 267 nm absorption is strong due to a 0–1 transition corresponding to an out of plane C–H bending mode. For indole, 0–0 transitions for the ^1L_b and ^1L_a states are at 285 and 274 nm respectively so a range of vibrational modes are excited at 267 nm.[53] As our laser has a bandwidth of 1 nm, we use an average over the laser wavelength range to derive the excitation cross sections presented in Table 1. Using these values, estimates for the ionization cross sections which fit the experimental data are also presented in Table 1.

Discussion

Let us now consider the laser pulse conditions required for real time detection of an aromatic molecule at a concentration of 1 pptv (part per trillion by volume) in air using REMPI. The ion production rate is given by eqn (7) multiplied by the laser repetition rate R. We make the assumption that a laser beam of full width half maximum D = 2 mm crosses a gas jet of width 2 mm and a density of 2×10^{14} cm^{-3} (such gas target conditions have been achieved previously[54]). Using toluene as an exemplar, if an ion production rate of 10 s^{-1} is required for close to real time detection, then the laser must satisfy the condition;

$$E^2 R > 0.001 \quad (8)$$

Therefore, for a laser operating at 1 kHz, a pulse energy greater than 1 mJ is required (or 0.3 mJ at 10 kHz). For the gas jet conditions described this corresponds to a limit of detection of a few attomoles.

As eqn (7) includes the assumption that any dynamics in the intermediate excited state does not alter the ionization probability, there is no dependence on the pulse length. However, this is not the case when we consider the yield of ions from air given by eqn (6). If we impose the constraint that the rate of ions generated from O_2 and N_2 must be no more than 10^4 s^{-1} in order to avoid detector saturation, the cross sections obtained in section 3 give the following condition;

$$\tau^2 > 10^{-17} E^3 R \quad (9)$$

which for a 1 kHz repetition rate, means the pulse length must be greater than 10 ps.

These laser conditions are readily satisfied by current solid-state laser systems based on Ti:sapphire (800 nm), Nd:YAG (1064 nm) or ytterbium doped crystals (1028 nm). Assuming 10% conversion of the fundamental into the 3rd (266/7 nm) or 4th harmonic (257 nm) respectively, a laser producing 10 mJ, >10 ps pulses at 1 kHz (10 W) would be capable of detecting toluene at the pptv level or sub pptv for indole in real time. While these types of laser systems are still mostly found in research labs, user friendly short pulse fibre and disc laser systems are approaching similar specifications.[55] With further optimization of the laser–gas interaction geometry[56] which could include multiple reflections of the laser through the target, these detection sensitivities could be reached with current commercial lasers which are compact, rugged, and modestly priced.

Conclusions

By measuring the ion yields of several gases irradiated with femtosecond laser pulses at a wavelength of 267 nm, we have measured single and multiphoton ionization cross sections for some exemplar gases. With these values we show that for aromatic organic molecules which are resonant at this wavelength, attomole detection limits can be achieved with ionization rates exceeding that of N_2 and O_2 sufficiently to facilitate real-time detection in air at 1 pptv concentrations. This could be achieved with currently available kHz picosecond laser systems producing energies of several mJ per pulse. As many of the organic molecules have chromophores which absorb in this wavelength range, particularly those of interest for health monitoring, this sensitivity of detection could open up trace detection of new biomarkers in breath, blood and biopsy analysis. As most drugs are also resonant at these wavelengths, there is further potential for applications in pharmacokinetics.[57]

Other organic molecules which absorb more weakly in this wavelength range will naturally require higher concentrations for identification. However, for ketones with excitation cross sections around 5×10^{-20} cm^2 at 267 nm,[58] this would still be an impressive 25 pptv. Alternatively shorter wavelengths available using the next laser harmonic (200, 206 or 213 nm) would enable resonant 1 + 1 ionization of most organic molecules. For those molecules with excited states which decay on ultrafast timescales, higher limits of detection can also be expected as the ionization is not as efficient. However, this can be mitigated through the use of femtosecond pulses,[23] albeit higher concentration levels would be required since ionization of the background gas will be more efficient.

Ultimately, the ideal laser system would be one which can produce wavelength tuneable picosecond pulses. A 10 ps pulse at 267 nm can in principal support a bandwidth of 2 cm^{-1} (0.01 nm), which can easily resolve vibrational structure in the absorption spectrum. Selection of absorption maxima would enhance the sensitivity, but by scanning the wavelength a two dimensional spectrum (mass *vs.* wavelength) could also be generated. This would be particularly valuable for identifying compounds in very complex mixtures, including isomers.[5–8] Further discrimination in the ionization stage can also be obtained using a two color scheme, as has been demonstrated in nitric oxide.[19]

By using circularly polarized pulses, this selectivity could be extended to identifying enantiomers through circular dichroism in the ion yields as has been demonstrated in some exemplar molecules.[59–63] Although this will be hard to achieve in practice as the circular dichroism is typically very small, the sensitivity would far outstrip conventional chiral detection methods. Given the prevalence of chirality in biological molecules and therapeutic drugs, a chiral-REMPI analysis instrument would be a powerful analytical tool.

In conclusion, with the rapid advances in laser technology, the opportunity for more widespread use of short pulse lasers combined with mass spectrometry for very high sensitivity trace analysis is becoming possible, particularly for health related applications. While the use of such lasers in bed-side monitoring devices is unlikely, there is potential for off-line analysis of breath, fluid or tissue samples which would offer much higher sensitivity than any other currently available analytical techniques.

Acknowledgements

This work was supported by the STFC Laser Loan Scheme, the Leverhulme Trust (grant RPG-2012–735), the UK's Engineering and Physical Sciences Research Council (grant EP/M001644/1). GA is supported by EPSRC's Doctoral Training Grant scheme, JM by the Northern Ireland Department of Employment and Learning. The participation of TJK and JTC was made possible by Science Foundation Ireland Grant no. 12/IA/1742.

Notes and references

1 U. Boesl, H. J. Neusser and E. W. Schlag, *Z. Naturforsch., A: Phys. Sci.*, 1978, **A33**, 1546–1548.
2 L. Zandee and R. B. Bernstein, *J. Chem. Phys.*, 1979, **71**, 1359–1371.
3 U. Boesl, H. J. Neusser and E. W. Schlag, *Chem. Phys.*, 1981, **55**, 193–204.
4 U. Boesl, *J. Mass Spectrom.*, 2000, **35**, 289–304.
5 L. Oudejans, A. Tuati and B. K. Gullett, *Anal. Chem.*, 2004, **76**, 2517–2524.
6 H. Oser, R. Thanner and H.-H. Grotheer, *Chemosphere*, 1998, **31**, 2361–2374.
7 M. Nomayo, R. Thanner and H.-H. Grotheer, *Appl. Phys. B*, 2000, **71**, 681–687.
8 H. Tsukatani, H. Okudaira, T. Uchimura and T. Imasaka, *Anal. Sci.*, 2009, **25**, 599.
9 B. K. Gullett, L. Oudejans, D. Tabor, A. Touati and S. Ryan, *Environ. Sci. Technol.*, 2012, **46**, 923–928.

10 R. Zimmermann, H. J. Heger, A. Kettrup and U. Nikolai, *Fresenius' J. Anal. Chem.*, 2000, **366**, 368–374.
11 B. K. Gullett, A. Touati and L. Oudejans, *Atmos. Environ.*, 2008, **42**, 2117–2128.
12 T. Streibel and R. Zimmerman, *Annu. Rev. Anal. Chem.*, 2014, **7**, 361–381.
13 M. Nomayo, R. Thanner and H.-H. Grotheer, *Appl. Phys. B*, 2000, **71**, 681–687.
14 S. Schmidt, M. F. Appel, R. M. Garnica, R. N. Schindler and T. Benter, *Anal. Chem.*, 1999, **71**, 3721–3729.
15 T. Streibel, K. Hafner, F. Műhlberger, T. Adam and R. Zimmermann, *Appl. Spect.*, 2006, **60**, 72–79.
16 R. Thanner, H. Oser and H.-H. Grotheer, *Eur. Mass Spectrom.*, 1998, **4**, 215–222.
17 Y. Deguchi, S. Dobashi, N. Fukuda, K. Shinoda and M. Morita, *Environ. Sci. Technol.*, 2003, **37**, 4737–4742.
18 T. Uchimura and T. Imasaka, *Anal. Chem.*, 2000, **72**, 2648–2652.
19 L. C. Short, R. Frey and T. Benter, *Appl. Spectrosc.*, 2006, **60**, 217–222.
20 H. Oser, S. E. Young and M. J. Coggiola, *Breath Analysis Using Photoionization Mass Spectrometry.*, SRI International Menlo Park, CA, USA, 2004.
21 A. Li, T. Uchimura, H. Tsukatani and T. Imasaka, *Anal. Sci.*, 2010, **26**, 841–846.
22 A. Li, J. Song, Y. Sun and T. Jiao, *J. Spectrosc.*, 2014, 134828.
23 S. Yamaguchi, T. Uchimura and T. Imasaka, *Anal. Sci.*, 2006, **22**, 1483–1487.
24 Y. Watanabe-Ezoe, X. Li, T. Imasaka, T. Uchimura and T. Imasaka, *Anal. Chem.*, 2010, **82**, 6519–6525.
25 Y.-. C. Chang and T. Imasaka, *Anal. Chem.*, 2013, **85**, 349–354.
26 R. Weinkauf, P. Aicher, G. Wesley, J. Grotemeyer and E. W. Schlag, *J. Phys. Chem.*, 1994, **98**, 8381–8391.
27 Y. Hashiguchi, S. Zaitsu and T. Imasaka, *Anal. Bioanal. Chem.*, 2013, **405**, 7053–7059.
28 K. W. D. Ledingham and R. P. Singhal, *Int. J. Mass Spectrom. Ion Processes*, 1997, **163**, 149–168.
29 J. Peng, N. Puskas, P. B. Corkum, D. M. Rayner and L. V. Loboda, *Anal. Chem.*, 2012, **84**, 5633–5640.
30 O. Kelly, M. J. Duffy, R. B. King, L. Belshaw, I. D. Williams, J. Sá, C. R. Calvert and J. B. Greenwood, *Analyst*, 2012, **137**, 64.
31 M. Liu, C. Wu, Z. Wu, H. Yang, Q. Gong, W. Huang and T. Zhub, *J. Am. Soc. Mass Spectrom.*, 2010, **21**, 1122–1128.
32 S. M. Hankin, D. M. Villeneuve, P. B. Corkum and D. M. Rayner, *Phys. Rev. Lett.*, 2000, **84**, 5082–5085.
33 J. Muth-Böhm, A. Becker and F. H. M. Faisal, *Phys. Rev. Lett.*, 2000, **85**, 2280–2283.
34 A. Jaroń-Becker and A. Becker, *Laser Phys.*, 2009, **19**, 1705–1711.
35 A. E. Boguslavskiy, J. Mikosch, A. Gijsbertsen, M. Spanner, S. Patchkovskii, N. Gador, M. J. J. Vrakking and A. Stolow, *Science*, 2012, **335**, 1336–1340.
36 A. Kucher, A. Wucher and N. Winograd, *J. Phys. Chem. C*, 2014, **118**, 25534–25544.
37 M. A. Turner, S. Bandelow, L. Edwards, P. Patel, H. J. Martin, I. D. Wilson and C. L. P. Thomas, *J. Breath Res.*, 2013, **7**, 017102.
38 D. Poli, P. Carbognani, M. Corradi, M. Goldoni, O. Acampa, B. Balbi, L. Bianchi, M. Rusca and A. Mutti, *Resp. Res.*, 2005, **6**, 71.
39 S. Kischkel, W. Miekisch, A. Sawacki, E. M. Straker, P. Trefz, A. Amann and J. K. Schubert, *Clin. Chim. Acta*, 2010, **411**, 1637–1644.
40 J. D. Alexander, L. Graham, C. R. Calvert, O. Kelly, R. B. King, I. D. Williams and J. B. Greenwood, *Meas. Sci. Technol.*, 2010, **21**, 045802.
41 Y. Itikawa, *J. Phys. Chem. Ref. Data*, 2006, **35**, 31–53.
42 J. R. Vacher, F. Jorand, N. Blin-Simiand and S. Pasquiers, *Chem. Phys. Lett.*, 2007, **434**, 188–193.
43 B. Trost, J. Stutz and U. Platt, *Atmos. Environ.*, 1997, **31**, 3999–4008.
44 T. Etzkorn, B. Klotz, S. Sörensen, I. V. Patroescu, I. Barnes, K. H. Becker and U. Platt, *Atmos. Environ.*, 1999, **33**, 525–540.
45 P. Sahay, S. T. Scherrer and C. Wang, *Sensors*, 2013, **13**, 8170–8187.
46 M. Yujing and A. Mellouki, *J. Photochem. Photobio., A*, 2000, **134**, 31–36.
47 S. Fally, M. Carleer and A. C. Vandaele, *J. Quant. Spectrosc. Radiat. Transfer*, 2009, **110**, 766–782.
48 K. C. Kulander, *Phys. Rev. A*, 1988, **38**, 778–787.
49 E. J. McGuire, *Phys. Rev. A*, 1981, **24**, 835.
50 R. S. Mangina, J. M. Ajello, R. A. West and D. Dziczek, *ApJ*, 2011, **196**, 1–34.
51 T. Etzkorn, *et al.*, *Atmos. Environ.*, 1999, **33**, 525.
52 J. E. Bartmess, J. F. Liebman, J. L. Holmes, R. D. Levin and W. G. Mallard, Ion Energetics Data in *NIST Chemistry WebBook, NIST Standard Reference Database Number 69*, ed. P. J. Linstrom and W. G. Mallard, National Institute of Standards and Technology, Gaithersburg MD, 20899, http://webbook.nist.gov, (retrieved January 15, 2015).
53 E. H. Strickland, J. Horwitz and C. Billups, *Biochem.*, 1970, **9**, 4914–4921.
54 M. F. Appel, L. C. Short and T. Benter, *J. Am. Soc. Mass Spectrom.*, 2004, **15**, 1885–1896.
55 Z. Yang, X. Hu, Y. Wang, W. Zhang and W. Zhao, *Chin. Opt. Lett.*, 2011, **9**, 041401.
56 T. Matsui and T. Imasaka, *Anal. Sci.*, 2014, **30**, 445–449.
57 J. Kleeblatt, S. Ehlert, J. Hölzer, M. Sklorz, J. Rittgen, P. Baumgärtel, J. K. Schubert and R. Zimmermann, *Appl. Spectrosc.*, 2013, **67**, 860–872.
58 M. Yujing and A. Mellouki, *Anal. Chim. Acta*, 2011, **694**, 108–114.
59 C. Loge, A. Bornschlegl and U. Boesl, *Anal. Bioanal. Chem.*, 2009, **395**, 1631.
60 P. Horsch, G. Ubasch and K.-M. Weitzel, *Chirality*, 2012, **24**, 68.
61 U. Boesl, A. Bornschlegl, C. Logé and K. Titze, *Anal. Bioanal. Chem.*, 2013, **405**, 6913.
62 A. Hong, C. M. Choi, H. J. Eun, C. Jeong, J. Heo and N. J. Kim, *Angew. Chem., Int. Ed.*, 2014, **53**, 7805–7808.
63 K. Titze, T. Zollitsch, U. Heiz and U. Boesl, *ChemPhysChem*, 2014, **15**, 2762–2767.